# Interference in Photo-detachment of tri-atomic negative ion near a hard reflecting surface

K. Farooq[1*], Habib U Rehman[1], S. M. Asif[1], M. Abbas Khan[2] , M. A. Khan[3]
[1] *Department of physics, Balochistan University of Information Technology, Engineering and Management Sciences (BUITEMS), Pakistan*
[2] *Department of Electrical engineering, Balochistan University of Information Technology, Engineering and Management Sciences (BUITEMS), Pakistan and*
[3] *Department of Physics, Khwaja Fareed University of Engineering and Information Technology, Rahim Yar Khan, Pakistan*

The phenomena in which an extra electron is removed from a negative ion is called photo-detachment. Photo-detachment is important phenomena, used to find the structure of anions, particulary to find the electron affinities. In this paper, we present theoretically the induced effects in the photo-detached of tri-atomic anion $H_3$ near hard reflecting wall or surface. For the photo-detachment process, a Z-polarized coherent source of radiations (laser) is used to kick electrons from $H_3$ like anion in the domain of a hard reflecting surface. Imaging method is adopted to derive the generalized detached electron wave, differential cross-section and the total cross-section Analytically. Numerical solutions (simulations) for total electron flux and the total cross-section is also presented. In the electron flux, shows visible oscillation and hence the induced effect of surface in the interference. It is depicted that the reflecting hard wall strongly affects the flux and total photo-detachment cross-section.

PACS numbers: 33.80.-b; 32.80.Gc; 32.80.Qk

Keywords: Photo-detachment; Interference.

## I. INTRODUCTION

Interference in microscopic system remained a focused and central topic of Modern physics and quantum mechanics. The quantum interference not only posses interesting physics but also having number of applications. Therefore, this amazing phenomena got great attentions both experimentally and theoretically. The associated waves packets with microscopic quantum systems investigated in the last century. In the area of experimental physics, Young's double slit experiment explains the interference effects in the electrons or microscopic particles in simple way. Same quantum interference is observed in photo-detachment of negative anions.

The physics of anions attracted attention in the last two decades. The phenomena of photo-detachment occurs in negative ions, used to investigate structure, wave nature determination, electron affinities, and hence leads to the microscopy of photo-detachment. The same microscopy of anions has been set itself to a very sensitive procedure for accurate measurements of electron affinities of negative atoms [1, 2]. The research work has been gifted with large numbers of publications about the photo-detachment [3–9]. In these studies, Bryant *et. al.* [3] observed a ripple-like patrons in total cross-section of hydrogen negative ions in the presence of static electric field ranging, whose range was from few hundred kV/cm above the threshold. Theoretically some papers were presented in order to explain these structure or ripple behaviors. In these studies the approach of frame transformation theory was used by Rau and wong [5], while the other two physicist Du and Delos [10–12] presented closed orbit theory to explanation these oscillatory behaviors.

The phenomena of Photo-detachment of negative ions was extended to the external fields [13–15]. As a number of external sources strongly effect the photo-detached electron spectra. The photo-detached spectrums switches from an oscillation [16–19] to smooth behaviors [20]. The photo-detachment mechanism was also considered in the presence of the surfaces i.e. some time called walls or the external environment. These surfaces can be categorized in the hard surfaces and the soft surfaces. In this domain the photo-detachment process of hydrogen ($H^-$) in the vicinity of a reflecting surface was considered by Yang et. al. They adopted closed-orbit theory[21]. The main result and contribution of the reflecting wall was the induced oscillation in the photo-detachment cross-section. Afaq and Du considered the photo-detachment of of hydrogen anion near a reflecting wall. They used the theoretical imaging

* farooq.khan@buitms.edu.pk

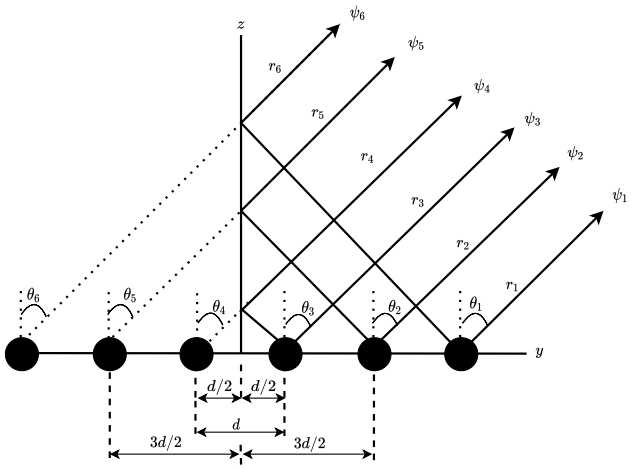


FIG. 1: The schematic diagram of the tri-atomic anion near the hard reflecting wall is considered. The anions are considered along the y-axis with separation d, while separated from the surface $\frac{d}{2}, \frac{3d}{2}$ and $\frac{5d}{2}$. The coherent laser source is incident along the z direction

.

method, quite different from the closed-orbit theory [22]. This method provided a tool to derive relations for photo-detachment cross-section.

Here in this research article, we consider photo-detachment in tri-atomic anion near hard reflecting surface using the theoretical imaging method. A coherent source of radiation is used for the photo-detachment process. The detached electron waves have two possibilities. One of which is the wave traveling directly while the other wave reflects from reflecting wall, with phase loss. We calculate the total detached electron wave and analytical formula for detached-electron flux. We consider the distributions of electron flux on a screen placed at a large distance from the negative ion system on a distant screen for different photon energies.

This article is organized as: in section II, models and calculations for theoretical study is presented. Total detached wave function and out going flux are given in section III. In the other section IV, the details of cross-section area is presented. For various experimental feasible values, discussion and conclusion are presented in section V. Atomic units will be used unless otherwise noted.

## II. MODELS AND CALCULATIONS

We consider a tri-atomic anion along the y-axis near a hard reflecting surface. A Z-polarized coherent source of laser light interacts with negative ions system as shown in the Fig.1. The hard reflecting surface is considered perpendicular to the Y-axis, while the negative ions are taken along the Y-axis. The negative ions are placed at distance $\frac{d}{2}$, $\frac{3d}{2}$ and $\frac{5d}{2}$ respectively from the the hard reflecting surface. The hard reflecting surface is placed at the origin, perpendicular to the y-axis such that the surface acts like a plane mirror, the images of negative ions are formed at the left side of the reflecting surface. The images are at same distance as the sources (at a distance $\frac{d}{2}$, $\frac{3d}{2}$ and $\frac{5d}{2}$) respectively from the the reflecting surface.

The laser light is incident along the z-axis on the tri-atomic anion normal to the anion axis. Then the photo-detachment phenomena occurred in: in first step, energy $E_{ph}$ of the photon is absorbed by an extra electron and take a trajectory from anion as a wave. In the next second step, the electron propagates through large distance. The electron wave may be generated from each system but with different phase. The interference of the outgoing waves occurs at a large distance and result into the oscillations in the electron flux.

Let $\psi_1$, $\psi_2$ and $\psi_3$ are the direct components moving along the path $r_1$, $r_2$ and $r_3$ respectively making angle $\theta_1$, $\theta_2$ and $\theta_3$ respectively with z-axis. The other component waves $\psi_4$, $\psi_5$ and $\psi_6$ initially towards the surface with an angle $(2\pi - \theta_4)$, $(2\pi - \theta_5)$ and $(2\pi - \theta_6)$ respectively, then after reflecting propagates along the path $r_4$, $r_5$ and $r_6$ respectively. The reflected waves appears to be originating from the images of the negative ions on the other side of the mirror or behind the hard surface/wall. In the absence of surface the detached waves $\Psi_1$, $\Psi_2$ and $\Psi_3$ are $\Psi_1 = Ccos\theta_1 \frac{exp(ikr_1)}{kr_1}$, $\Psi_2 = Ccos\theta_2 \frac{exp(ikr_2)}{kr_2}$, and $\Psi_3 = Ccos\theta_3 \frac{exp(ikr_3)}{kr_3}$.

Here, $C = \frac{4kBi}{(k_b^2+k^2)^2}, k = (2E)^{\frac{1}{2}}, k_b = 2E_b$ while E is related to energy of the detached electron, and $k_b$ is connected to $E_b$ the binding energy of the negative ion i.e. can be written as $E_b = \frac{k_b}{2}$. The normalization constant $B = 0.31552$.

Similarly the propagating detached electron waves in the direction $(2\pi - \theta_4)$, $(2\pi - \theta_5)$ and $(2\pi - \theta_6)$ the reflected components of waves $\psi_4$, $\psi_5$, and $\psi_6$ are obtained. Due to hard reflecting surface an additional phase $\mu\frac{\pi}{2}$ contributes in reflected components. Theses reflected component $\psi_4$, $\Psi_5$ and $\psi_6$ can be written as,

$\Psi_4 = Ccos(2\pi - \theta_4)\frac{expi(kr_4 - \mu\frac{\pi}{2})}{kr_4}$, $\Psi_5 = Ccos(2\pi - \theta_5)\frac{expi(kr_5 - \mu\frac{\pi}{2})}{kr_5}$ and $\Psi_6 = Ccos(2\pi - \theta_6)\frac{expi(kr_6 - \mu\frac{\pi}{2})}{kr_6}$.

Here $\mu$ is called Maslov indices, classify the nature of the reflecting surface. Here we consider $\mu = 2$ for hard case. In the next section, we'll calculate the total detached electron flux.

## III. TOTAL DETACHED WAVE FUNCTION AND ELECTRON FLUX

When laser light of suitable energy is incident on the negative ions, electrons are ejected from the negative ion. These waves propagate in all the direction i.e. spread like a sphere in all directions. We assume that $r, \theta, \phi$ be the entire spherical polar coordinates. Using superposition principle, the total out going wave function is

$$\Psi_{(r,\theta,\phi)} = \frac{1}{\sqrt{6}}[\Psi_1 + \Psi_2 + \Psi_3 + \Psi_4 + \Psi_5 + \Psi_6]. \tag{1}$$

Using the corresponding relations in the above equation we reach to,

$$\Psi_{(r,\theta,\phi)} = \frac{1}{\sqrt{6}}[Ccos\theta_1\frac{exp(ikr_1)}{kr_1} + Ccos\theta_2\frac{exp(ikr_2)}{kr_2} + Ccos\theta_3\frac{exp(ikr_3)}{kr_3} + Ccos(2\pi - \theta_4)\frac{exp(i(kr_4 - \mu\frac{\pi}{2}))}{kr_4} + Ccos(2\pi - \theta_5)\frac{exp(i(kr_5 - \mu\frac{\pi}{2}))}{kr_5} + Ccos(2\pi - \theta_6)\frac{exp(i(kr_6 - \mu\frac{\pi}{2}))}{kr_6}] \tag{2}$$

Here, we assumed the six components of detached electrons waves, which propagate through a large distance. The trajectories of these detached waves components to be $r_1, r_2, r_3, r_4, r_5$, and $r_6$.To derive the expression for total detached electron waves (electron flux), we us large distance approximation $r_1 \approx r - \frac{5kdsin\theta sin\phi}{2}$, $r_2 \approx r - \frac{3kdsin\theta sin\phi}{2}$, $r_3 \approx r - \frac{kdsin\theta sin\phi}{2}$, $r_4 \approx r + \frac{kdsin\theta sin\phi}{2}$, $r_5 \approx r + \frac{3kdsin\theta sin\phi}{2}$ and $r_6 \approx r + \frac{5kdsin\theta sin\phi}{2}$. These approximations are used only in phase terms while in all other terms, use $r_1 \approx r_2 \approx r_3 \approx r_4 \approx r_5 \approx r_6 \approx r$, and $\theta_1 \approx \theta_2 \approx \theta_3 \approx \theta_4 \approx \theta_5 \approx \theta_6 \approx \theta$. Using $\mu = 2$, then the wave functions are given as

$$\psi_1 = Ccos\theta\frac{exp(i(kr - \frac{5kd\sin\theta\sin\phi}{2})}{r}$$

$$\psi_2 = Ccos\theta\frac{exp(i(kr - \frac{3kd\sin\theta\sin\phi}{2})}{r}$$

$$\psi_3 = Ccos\theta\frac{exp(i(kr - \frac{kd\sin\theta\sin\phi}{2})}{r}$$

$$\psi_4 = Ccos\theta\frac{exp(i(kr + \frac{kd\sin\theta\sin\phi}{2}) - \frac{2\pi}{2})}{r}$$

$$\psi_5 = Ccos\theta\frac{exp(i(kr + \frac{3kd\sin\theta\sin\phi}{2}) - \frac{2\pi}{2})}{r}$$

$$\psi_6 = Ccos\theta\frac{exp(i(kr + \frac{5kd\sin\theta\sin\phi}{2}) - \frac{2\pi}{2})}{r} \tag{3}$$

Using the above relations in Eq.1, we reach to the following result,

$$\Psi_{(r,\theta,\phi)} = \frac{2}{\sqrt{6}} C\cos\theta[sin(\frac{5kd\sin\phi\sin\theta}{2}) + sin(\frac{3kd\sin\phi\sin\theta}{2}) + sin(\frac{kd\sin\phi\sin\theta}{2})](\frac{exp^{i(kr-\frac{\pi}{2}}}{r}) \tag{4}$$

The electron flux is given by [24],

$$J_{(r,\theta,\phi)} = \frac{i}{2}(\Psi\nabla\Psi^* - \Psi^*\nabla\Psi)$$

$$J_{(r,\theta,\phi)} = \frac{2kC^2cos^2\theta}{3r^2}[(\sin\alpha + \sin\beta + \sin\gamma)^2] \tag{5}$$

The representations are $\alpha = \frac{5kd\sin\phi\sin\theta}{2}$, $\beta = \frac{3kd\sin\phi\sin\theta}{2}$, and $\gamma = \frac{kd\sin\phi\sin\theta}{2}$

$$\begin{aligned} J_{(r,\theta,\phi)} = \frac{2kC^2cos^2\theta}{3r^2}[&\frac{3}{2} - \frac{1}{2}\cos(5kd\sin\phi\sin\theta) - \frac{1}{2}\cos(3kd\sin\phi\sin\theta) - \frac{1}{2}\cos(kd\sin\theta\sin\phi) \\ &+2\sin(\frac{5kd\sin\phi\sin\theta}{2})\sin(\frac{3kd\sin\phi\sin\theta}{2}) + 2\sin(\frac{5kd\sin\theta\sin\phi}{2})\sin(\frac{kd\sin\phi\sin\theta}{2}) \\ &+2\sin(\frac{3kd\sin\phi\sin\theta}{2})\sin(\frac{kd\sin\phi\sin\theta}{2})]. \end{aligned} \tag{6}$$

The detached electron flux at any point $\rho = \sqrt{x^2+y^2+z^2}$ or $r = \sqrt{x^2+y^2+z^2}$ on the screen placed in the XY-plane at a distance L, which is at z=L from the system is

$$\begin{aligned} J_z(\rho) = \frac{kC^2L^3}{(x^2+y^2+z^2)^{5/2}}[&1 - \frac{1}{3}\cos(\frac{5kdy}{\sqrt{x^2+y^2+z^2}}) - \frac{1}{3}\cos(\frac{3kdy}{\sqrt{x^2+y^2+z^2}}) - \frac{1}{3}\cos(\frac{kdy}{\sqrt{x^2+y^2+z^2}}) \\ &+\frac{4}{3}\sin(\frac{5kdy}{2\sqrt{x^2+y^2+z^2}})\sin(\frac{3kdy}{2\sqrt{x^2+y^2+z^2}}) + \frac{4}{3}\sin(\frac{5kdy}{2\sqrt{x^2+y^2+z^2}})\sin(\frac{kdy}{2\sqrt{x^2+y^2+z^2}}) \\ &+\frac{4}{3}\sin(\frac{3kdy}{2\sqrt{x^2+y^2+z^2}})\sin(\frac{kdy}{2\sqrt{x^2+y^2+z^2}})]. \end{aligned} \tag{7}$$

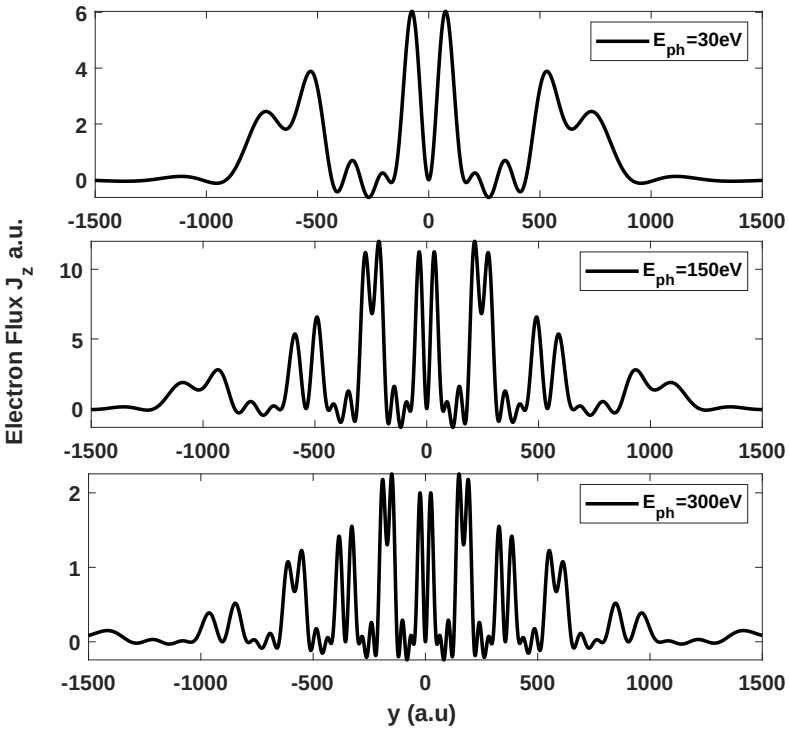


FIG. 2: The out going flux given in Eq.(7), is plotted versus Y. The incident photon energies are given as (a) $E_{ph} = 30eV$, (b) $E_{ph} = 150eV$, and (c) $E_{ph} = 300eV$, while L=1000 a.u. and interatomic distance d=4 a.u.

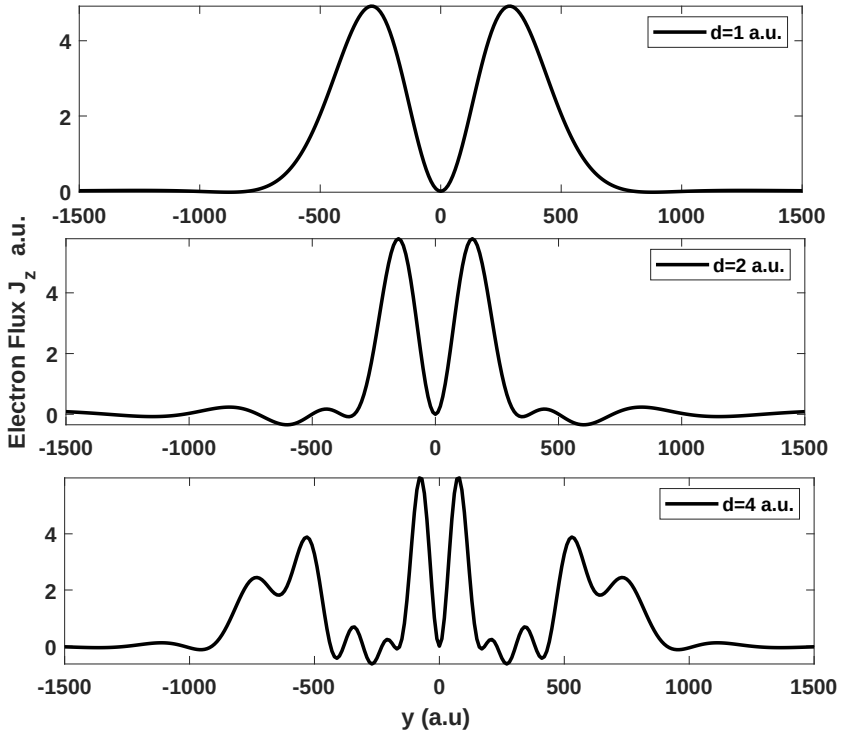


FIG. 3: The out going flux given in Eq.(7), is plotted versus Y. The incident photon energy is $E_{ph} = 30eV$ while the interatomic distance is (a) d=1 a.u. (b) d= 2 a.u. and (c) d=4 a.u. while L=1000 a.u.

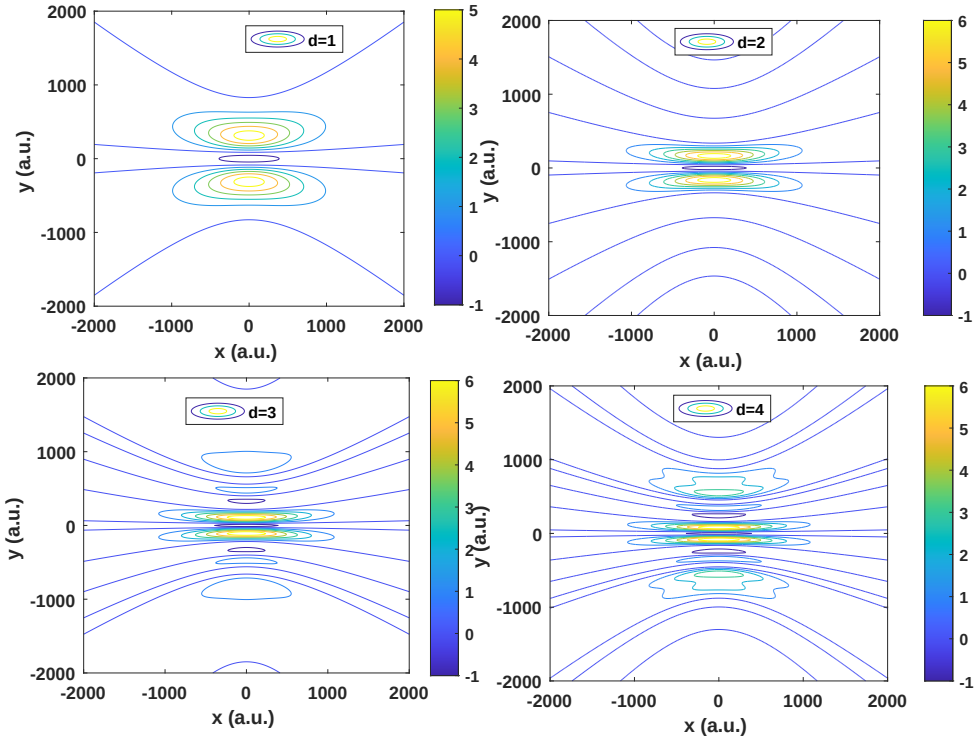


FIG. 4: The out going detached flux given in Eq.(7), shown in the contour plots. The incident photon energy is $E_{ph} = 30eV$ while the interatomic distance is (a) d=1 a.u. (b) d= 2 a.u. and (c) d=3 a.u. and (d) d=4 a.u. while L=1000 a.u.

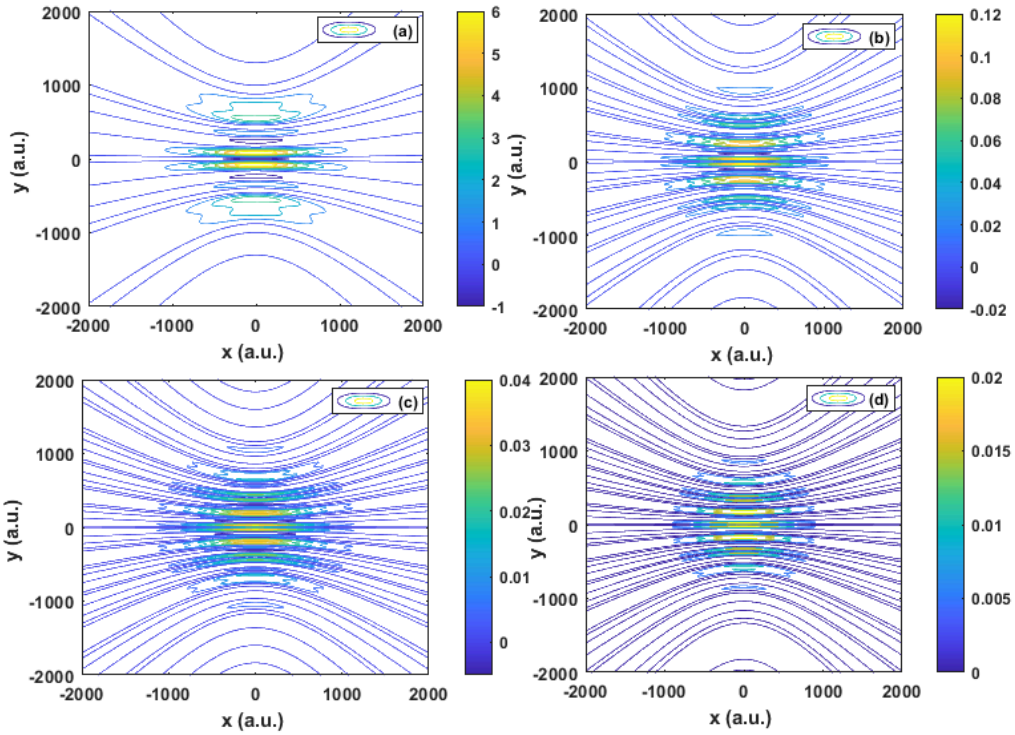


FIG. 5: The detached electron flux given in Eq.(7), shown in the contour plots. The incident photon energies are given as (a) $E_{ph} = 30eV$, (b) $E_{ph} = 150eV$, (c) $E_{ph} = 240eV$ and (d) $E_{ph} = 300eV$, while L=1000a.u and interatomic distance d=4 a.u.

The out going electron flux at x=0 on the screen using Eq.(7) are shown in the figures from Fig:2 to Fig:5, for various experimental values of incident energy $E_{ph}$, and inter atomic distances. Different interference plots are obtained. By increasing the photon energy,the peaks in the flux distribution also increases.

## IV. CROSS-SECTION AREA

For the total photo-detachment cross-section, a large hypothetical spherical surface Γ enclosing the negative ion system is considered. A generalized differential cross-section $d\sigma(q)/ds$ can be used to find the total photo-detachment cross section. The given realtion can be considered as [22],

$$\frac{d\sigma(q)}{ds} = \frac{2\pi E_{ph}}{c} j_r.n \tag{8}$$

Here, the speed of light is c measured in a.u. , and $ds = r^2 \sin\theta d\theta d\phi$. Now integrating the above equation to yields the overall cross-section,

$$\sigma(q) = \int \frac{d\sigma(q)}{ds} ds. \tag{9}$$

$$\sigma = \int \frac{2\pi E_{ph} j_r.n}{c} ds \tag{10}$$

Solving the above equation, we reached to the relations for the total cross-section as

$$\sigma = \sigma_0[1 + A_c + A_s + A_{cs}] \tag{11}$$

Here $\sigma_0 = \frac{8\pi^2 E_{ph} K C^2 E_{ph}}{3c}$, $A_c = \frac{\cos(5kd)}{(5kd)^2} + \frac{\cos(4kd)}{8(kd)^2} + \frac{3\cos(3kd)}{(3kd)^2} - \frac{3\cos(kd)}{(kd)^2}$ ,$A_{cs} = \frac{-cos(kd)\sin(kd)}{2(kd)^3}$ and $A_s = \frac{-\sin(5kd)}{(5kd)^3} - \frac{\sin(4kd)}{32(kd)^3} - \frac{\sin(3kd)}{9(kd)^3} + \frac{\sin(2kd)}{4(kd)^3} + \frac{3\sin(kd)}{(kd)^3}$.

## V. DISCUSSIONS AND CONCLUSION

In the current study, we focused on total detached electron wave function, the electron flux, and total photo-detachment cross-section. Out going total wave function is obtained in the Eq.4, calculated by the superposition principle and using set of Eqs.3. In this set of equations both the waves i.e. direct components and reflected components from the mirror images or reflected waves are used. In the total wave function, there is shift in the phase $\frac{\pi}{2}$. From the detached total wave the electron flux is calculated in the spherical polar coordinates. The electron flux in the cartesian coordinates system are calculated analytically in eq.7, which is one of the basic result of the current study. This relations is used to find the interference phenomena. For the interference phenomena the tuning parameter i.e. incident photon energy and the geometrical shape the interatomic distance are the prime interest. Using Eq.7.,the electron flux are plotted. In Fig.2 at x = 0, keeping the value of d = 4 a.u. constant, L = 1000a.u. and changing the incident photon energy which are $E_{ph}$ = 30eV, $E_{ph}$ = 150eV, and $E_{ph}$ = 300eV, different plots are obtained. These plots show that the surface has induced oscillation in the detached electron flux, by increasing the value of photon energy the oscillations increases.

In Fig.3 at x = 0, keeping fix the photon energy $E_{ph}$ = 30eV, while changing the interatomic distance d = 1 a.u., d = 2 a.u., and d = 4 a.u. obtained the plots. These plots show that the surface has induced oscillation in the detached electron flux, which increases with the increase in interatomic distance.

In Fig. 4 the electron flux in contour plots are shown, fixed the value of photon energy , which is $E_{ph} = 30eV$, while the interatomic distance are (a) d=1 a.u. (b) d= 2 a.u. and (c) d=3 a.u. and (d) d=4 a.u. In Fig. 5 the electron flux in contour plots are shown, by changing the incident photon energies as (a) $E_{ph} = 30eV$, (b) $E_{ph} = 150eV$, (c) $E_{ph} = 240eV$ and (d) $E_{ph} = 300eV$, while L=1000 a.u. and interatomic distance d=4 a.u. fixed. At low energy the electron wave have lower chance to interfere, hence lower the oscillations. As the energy increases, the number of oscillation increase, and maximum interference. At larger incident photon energy greater the inter-atomic distance, will cause maximum interference, the number of oscillations increases. The contour plots show that at d=1 the graphs are symmetrical. It shows that at smaller inter-atomic distance the phase shift does not effect the inference patterns, because of low path difference. When the inter-atomic distance increases the phase shift will contribute effectively

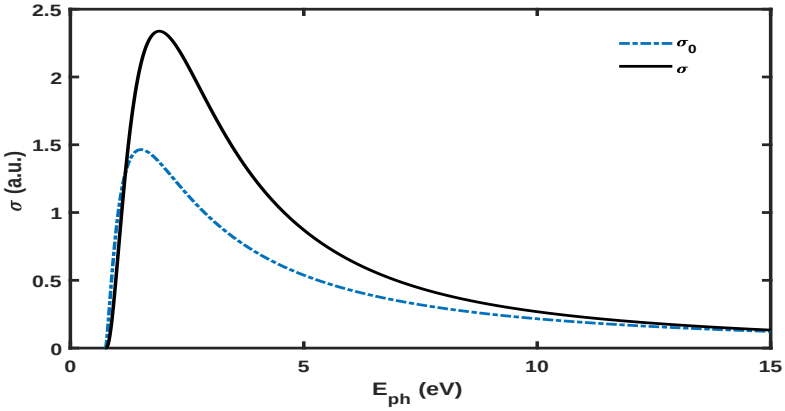


FIG. 6: Detached electron flux are plotting the value of photon energy is $E_{ph} = 30ev$, and keeping other parameters constant mention in figure i.e value of d=4 and L=1000.

and the interference patterns are more ripple like patterns.

Using Eq. (10), the total cross-section is calculated analytically and presented in Eq.11. The photo-detachment cross section is plotted against the photon energy in Fig.6. The doted line shows the cross-section of single negative ion without reflecting surface, while the smooth line shows the total cross section of tri-atomics anion in the presence of the reflecting surface. The total cross section shows a smooth behaviors. At larger atomic distance and lower photon energy limit, the total cross-section increases. While when $kd \simeq \infty$ then $A_c$, $A_s$ and $A_{cs} \simeq 0$. Then in Eq.12 $\sigma = \sigma_0$, which will confirmed in Fig:6, i.e. at larger photon energy the two plots coincides.

In conclusion, the photo-detachment of ti-atomic anion near to hard reflecting surface or wall is studied theoretically by using imaging method. This technique makes possible to derive formulae for the differential and as well as total cross sections in a straightforward way. It is shown that in the presence of reflecting surface the oscillations are induced in the differential cross-sections or electron flux. The phase of oscillation depends on the phase loss consider for the reflecting surface. In addition the dependence on photon energy and the distance between the negative shows that in interference the number of oscillations increases with the incident photon energy, and interatomic distance. The total photo detachment cross section is smooth, shows no visible oscillating behaviors.

[1] C. Blondel, C. Delsart, and F. Goldfarb, J. Phys. B: At. Mol. Opt. Phys 34 (2001) L281.
[2] C. Blondel, C. Delsart, C. Valli, et al,, Phys. Rev. A 64 (2001) 052504.
[3] Bryant H C *et al* 1987 Phys. Rev. Lett. **58** 2412
[4] Steward J E 1988 Phys. Rev. A **38** 5628
[5] Rau A R P and Wong H 1988 Phys. Rev. A **37** 632
[6] Du M L and Delos J B 1988 Phys. Rev. A **38** 5609
[7] Du M L 1989 Phys. Rev. A **40** 4983
[8] Peters A D *et al* 1997 Phys. Rev. A **56** 331
[9] Fabrikan I 2002 Phys. Rev. A **66** 010703(R)
[10] Du M L and Delos J B 1987 Phys. Rev. Lett. **58** 1731
[11] Du M L and Delos J B 1988 Phys. Rev. A **38** 1896
[12] Du M L and Delos J B 1988 Phys. Rev. A **38** 1913
[13] Wang D H, Li S S and Mu H F 2012 J. Phys. Soc. Japan 81 074301
[14] Wang D H, Wang S S and Tang T T 2011 J. Phys. Soc. Japan 80 094301
[15] Wang D H, Li S S, Wang Y H and Mu H F 2012 J. Phys. Soc. Japan 81 114301
[16] Arif S, Haneef M, Akbar J, Mohammad S, Ullah I, Khan H, Shah N, Zahir M and Rab A 2012 J. Kor. Phys. Soc.61 667
[17] Liu T Q, Hua W D, Cai H, Jiang L, Liang D Q and Cheng X S 2012 Chin. Phys. B 21 043401
[18] Haneef M, Ahmad I, Afaq A and Rahman A 2011 J. Phys. B: At. Mol. Opt. Phys. 44 195004
[19] Haneef M, Alam F E, Bakhtawar and Akbar J 2016 J. Phys.Soci. Japan 85 054302
[20] Haneef M, Ahmad I, Afaq A and Rahman A 2012 Chin. Phys. Lett. 29 013202
[21] Yang et al 2006 J. Phys. B: At. Mol. Opt. Phys. 39 1855
[22] A Afaq and M L Du J. Phys. B: At. Mol. Opt. Phys. 40 (2007) 13091321
[23] De-hua Wanga, Xin-yue Sun, and Tong Shi Eur. Phys. J. D (2019) 73: 15
[24] A. Afaqa, K. Farooqb, M. A. Khanb, and Yi Xue-Xi. Chin. Phys. B Vol. 23, No. 10 (2014) 103304